

PALEOPRODUCTIVITY OF OCEANIC UPWELLING AND THE EFFECT ON ATMOSPHERIC CO₂
AND CLIMATIC CHANGE DURING DEGLACIATION TIMES

Michael Sarnthein, Kyaw Winn and Rainer Zahn

Geological-Palaeontological Institute
Christian Albrecht University
Olshausenstr. 40
2300 Kiel
Federal Republic of Germany

ABSTRACT. In addition to variations in the Earth's orbit, changes in atmospheric pCO₂ represent an important factor in creating global climatic and ice volume changes. Atmospheric pCO₂ fluctuations are largely controlled by the exchange rates of CO₂ between the atmosphere and ocean reservoirs, an exchange which greatly depends upon plankton primary productivity in oceanic upwelling regions, where the carbon to carbonate "Rain Ratio" (Berger and Keir, 1984) is high. In order to test this model, a new equation to calculate the local ocean paleoproductivity has been developed. The formula is based on the relationships between carbon accumulation rate, water depth, and carbon-free bulk sedimentation rates (as a "sealing factor") of deep-sea sediments, and is independent of a large range of bottom water O₂ concentration. For comparison with paleoproductivity, $\delta^{13}\text{C}$ fluctuations of *Cibicidoides wuellerstorfi* serve to record the total CO₂ dissolved in North Atlantic Deep Water (NADW). In the region of coastal upwelling off northwest Africa, paleoproductivity increased by a factor of three from interglacial to glacial stages depicting a clear 100,000 year cycle. In oceanic "deserts", the productivity varied much less, but approximately with the same cycle during the last 0.5 my. Phase relationships during the last two Terminations show that trade wind strength and related productivity due to upwelling in the east Atlantic started to decrease slightly prior to or simultaneously with global ice melting, synchronously with a drastic increase in atmospheric pCO₂ (after Neftel et al., 1982). On the other hand, CO₂ depletion in the NADW only followed after some 2500 to 4500 years, and thus, cannot have caused the change in atmospheric CO₂. The high latitude insolation balance which causes changes in sea-ice cover and thus, of meridional trade wind intensity, is regarded as the prime factor responsible for this massive feedback mechanism for climatic change.

INTRODUCTION: EXTERNAL CAUSES OF CLIMATIC CHANGE

There is general agreement that a significant share of global climatic variance as monitored by oxygen-isotope curves can be explained by the Earth's orbital forcing according to the Milankovitch theory.

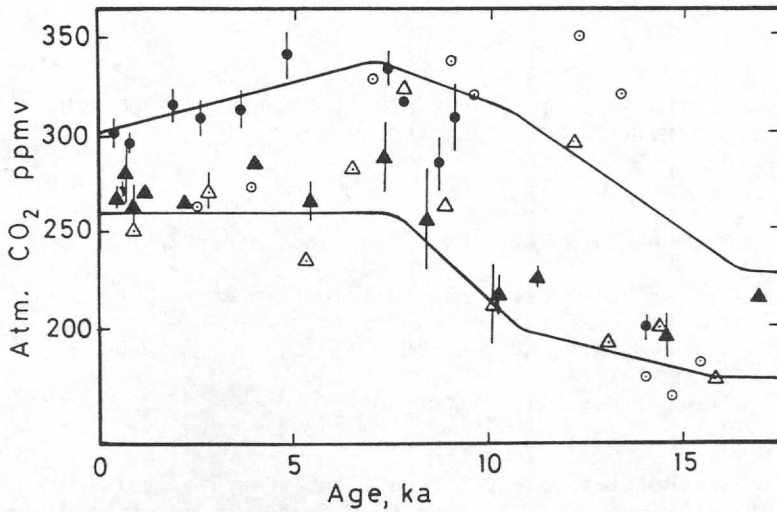


Figure 1. Ice core evidence for a change in atmospheric CO_2 during deglaciation. Circles: Greenland cores. Triangles: Antarctic cores. Open: Delmas et al. (1980). Filled with bounding line: Neftel et al. (1982). After Berger and Keir (1984).

ever, the extent of a linear response to orbital forcing is still under debate. Estimates vary, for example, from 15-25% (Herterich and Sarnthein, 1984) up to 77% (Imbrie et al., 1984). The residual climatic variance, whether small or large, requires consideration of stochastic mechanisms (Hasselmann, 1976) and also, a search for other (non-linear) external forcings unrelated to celestial mechanisms such as the effect of ice isostasy (e.g., Peltier and Hyde, 1984). This is especially true for an explanation of the 100,000-year cycle which is not yet well understood.

Within this context, the ice-core evidence of Delmas et al. (1980) and Neftel et al. (1982) provided a crucial breakthrough. They showed a major change in atmospheric pCO_2 from about 200 to about 300 ppmv during the last deglaciation (Fig. 1). Similar rate changes can be postulated also for earlier Terminations. Accordingly, CO_2 may have been essential in providing the required additional external forcing to accomplish climatic change by means of the "greenhouse effect" (Arrhenius, 1896). The ice core data of global change stimulated a series of studies searching for equivalent CO_2 changes in the ocean as recorded in deep-sea sediments (e.g. Duplessy et al., 1982, 1984; Shackleton et al., 1983; Boyle, 1986). In addition, a number of reservoir models arose, trying to tie this change to large scale processes that might vary the CO_2 exchange rates between the atmosphere and the oceanic deep water. This deep water is the main CO_2 reservoir containing at least 60 times more CO_2 than the atmosphere (Grassl et al., 1984). Broecker (1982; revoked 1984) regarded the nutrient inventory of P and N in the ocean as the limiting factor for CO_2 extraction from the atmosphere. More recently, Broecker

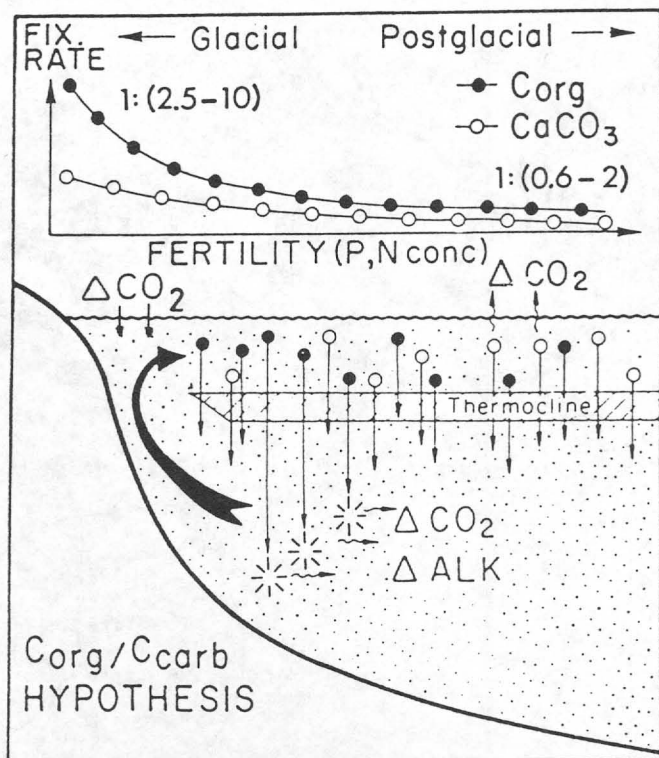


Figure 2. The carbon/carbonate Rain Ratio Model of Berger and Keir (1984).

et al. (1985) and Boyle and Keigwin (1985) considered the intensity of North Atlantic Deep Water (NADW) formation as the main control of differing CO_2 pressure in the atmosphere.

Siegenthaler and Wenk (1984) and Berger and Keir (1984) recognized the possible key role of changes in ocean surface circulation causing ocean productivity changes and thus affecting the atmospheric pCO_2 . Berger and Keir (1984) related the influence of productivity on CO_2 to the particle composition ("rain ratio") of plankton fluxes from the surface ocean to the deep sea (Fig. 2). This "biological pump" results in an annual bulk transfer of 23×10^9 tons of carbon from the sea surface (and the atmosphere) to greater water depths. The plankton "Rain Ratio Model" of Berger and Keir (1984) is based on data from various sediment traps. These data show that the ratio of organic carbon to carbonate carbon fixed in the particulate plankton flux varies systematically. The ratio increases from 0.6-2.0 below low-fertility areas to 2-10 below high-fertility areas such as zones of oceanic upwelling (Fig. 3a). In the high-fertility regions, the CO_2 extracted from the ocean deep-water by CaCO_3 dissolution is by far overcompensated by CO_2 produced by the

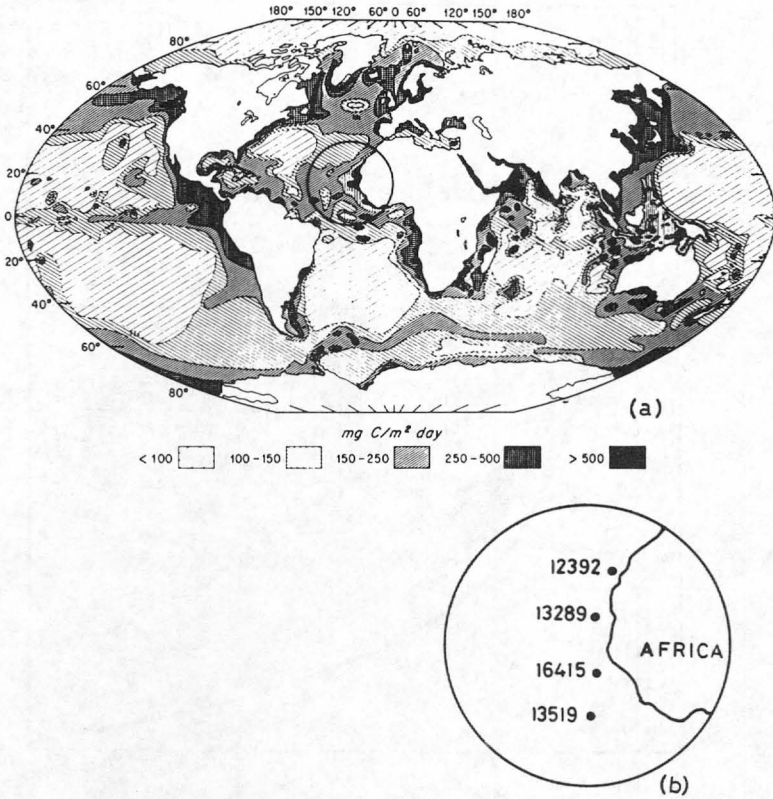


Figure 3. (a). Distribution of primary production in the World Ocean (After Koblentz-Mishke et al. 1970). (b). Core locations offshore from West Africa.

oxidation of carbon particles. On the other hand, CO_2 extraction should equal or exceed CO_2 production below low-fertility regions. In summary, intensity changes of surface-ocean productivity in upwelling zones may rule both the drawdown of total CO_2 by photosynthesis and the amount of CO_2 dissolved or extracted in the deep ocean. This model was also suggested by Flohn (1983) based on modern climate data.

The Rain Ratio Model (P. Weyl in Broecker, 1982) also predicts a change in the proportion of ^{12}C in total CO_2 dissolved in the deep ocean, because organic carbon is isotopically much lighter than dissolved carbon. Until now, however, the Rain Ratio Model has been supported by little hard data; this lack of data also applies to the other CO_2 models. The only direct multiseasonal measurements made in the modern equatorial Atlantic show that the carbon (and CO_2) transfer between the atmosphere and the ocean varies in a small-scale and uneven regional pattern. High carbon fluxes from the atmosphere to the ocean occur in

high productivity belts and are largely balanced by a reverse carbon flux outside of these belts (Oudot and Andrie, 1986).

In the present study, we compare partly new data of oceanic paleo-productivity with the benthos ^{13}C record of CO_2 variations in the ocean. Our evidence is obtained from two sediment cores from the East Atlantic, one from a high, the other from a low fertility region (Fig. 3b). In order to test the rain-ratio idea, we compare the phase relationships of paleoproductivity and deep-water oxygenation with that of the benthos oxygen-isotope record of global ice-volume change during the last and penultimate deglaciations (Terminations I and II), and finally, with the aeolo-marine sediment record of paleo-wind strength.

METHODS AND THEORY

The $\delta^{18}\text{O}$ record

The ratio of ^{18}O to ^{16}O has been measured in 1 to 20 specimens of the benthic foraminifera species *Cibicidoides wuellerstorfi* (315-400 μm) and is reported with respect to the international standard PDB as $\delta^{18}\text{O}$ in parts per thousand (‰). The data have been measured partly on a VG 602D micromass spectrometer (most values of core 13519; derived from Sarnthein et al., 1984) and partly on a Finnigan MAT 251 mass spectrometer combined with a new, fully automated carbonate preparation line (^{14}C Laboratory, Kiel University, Dr. H. Erlenkeuser and Finnigan Bremen, Dr. K. Habfast). A small part of the data set of core 12392 has been derived from Shackleton (1977) (for further details see Zahn et al., 1986).

The downcore variations in benthos $\delta^{18}\text{O}$ are largely related to the changing oceanic isotope composition as caused by the waxing and waning of the great Pleistocene ice sheets (Shackleton and Opdyke, 1973; Duplessy et al., 1985), fluctuations which serve as a standard of global climate history.

The paleoproductivity record

Equatorial and neritic upwelling areas and subpolar regions account for some 45%, and inshore waters for another 20% of the present-day global primary productivity of organic carbon in the world ocean (Koblentz-Mishke et al., 1970) (Fig. 3a). Therefore, a major portion of the CO_2 transfer from the surface to the deep ocean is confined to small parts of the ocean. This regionally-constrained CO_2 transfer was recently confirmed by the direct measurements of Oudot and Andrie (1986). Platt and Harrison (1985) demonstrated that actually only about one third of the total production is new production and the rest is regenerated production. Because of a lack of pertinent global data for new production, this difference has to be kept in mind when paleoproductivity numbers are calibrated in the following text with modern values of total primary production (Table II).

Müller and Suess (1979) were the first to present principles for tracing a productivity distribution pattern back into the past.

Specifically, they described a means to measure ancient values of primary (new!) productivity, i.e. the "paleoproductivity" in (deep-sea) sediments. Their paleoproductivity estimates were based on two variables: (1) the accumulation rates of organic carbon (C_A) as derived from the bulk sedimentation rate (S_B); the percentage of organic carbon (C), the porosity (Φ); and the density (ρ); and (2) the bulk sedimentation rates (S_B) which represent the burial rate, a sealing effect for organic carbon.

The argument that the two variables C_A and S_B may mathematically be *a priori* correlated (Müller and Suess, 1979, p. 1354) is incorrect because the sedimentation rates of organic carbon ($S_C = S_B \%C$) contained in C_A account for only a negligible proportion (mostly less than 1-3%) of the bulk-sedimentation rates (S_B). However, strictly speaking, the organic carbon free bulk-sedimentation rates (S_{B-C}) should be applied for defining the sealing effect. Pedersen (1983) confirmed by means of the iodine-bromine ratio in organic matter that the estimates of Müller and Suess (1979) are not simply a product of diagenetic effects acting on the organic carbon content, but indeed depict paleoproductivity.

The organic carbon accumulation rate (C_A) in the sediments used for calculating paleoproductivity is a function of the carbon flux near the sea floor (F_C), which in turn is a result of the primary production (P) and the water depth (z). As shown by Suess (1980), the relationship between primary production, carbon flux and water depth is non-linear because carbon consumption occurs at any given depth in the ocean below the euphotic zone, i.e.,

$$(1) F_C = kP^a z^b$$

and

$$\log F_C = \log k + a \log P + b \log z$$

or

$$(2) a \log P = \log F_C - \log k - b \log z$$

where k, a and b are constants. Subjecting the original (corrected and supplemented by recent data; Table I) data of Suess (1980) to multivariate analysis and applying a least squares fit for the carbon flux in equation (2), we obtain the following equation:

$$P = 4.90 F_C^{0.66} z^{0.32}$$

or

$$(3) F_C = \bar{P}^{1.5} / 11.11 z^{0.5} \quad (n=38; r=0.96; z \geq 50)$$

This water-depth relationship is fairly similar (for realistic water depths) to an equation published by Betzer et al. (1984) who also used a modified data set of Suess (1980).

$$(4) F_C = P^{1.41} / 2.44 z^{0.63}$$

Equation (3) was used for deducing an improved paleoproductivity equation. Essentially, we based our new equation on the old data set of Müller and Suess (1979) (Table II). However, we recalculated all sedimentation-rate data because new ^{14}C ages are now available for many cores. In addition, new equations which quantify the effects of vertical mixing by bioturbation were incorporated (Berger and Johnson, 1978; Erlenkeuser, 1980). Moreover, a set of recent core data from the equatorial east Atlantic (Tiedemann, 1985) and from the Pacific (Reimers and Suess, 1983a, b; Emerson, 1985) was added. Altogether, data from a total of 39 sites are compiled in Table II. In this set the eastern Atlantic is somewhat overrepresented because only twenty complete core data sets were available from elsewhere.

In summary, organic carbon accumulation rates C_A are a function of paleoproductivity (P) and water depth (equation 3), and of the ("sealing factor") bulk sedimentation rates (S_{B-C}):

$$(5) \quad C_A = k F_C S_{B-C}^a$$

Substituting equation (3) for F_C we arrive at:

$$C_A = k \frac{P^{1.5}}{11.11 z^{0.5}} S_{B-C}^a$$

or

$$(6) \quad 11.11 C_A z^{0.5} P^{-1.5} = k S_{B-C}^a$$

where a and k are constants. Linear regression analysis using the data set of Table II then yields $a = 1.08$ and $k = 0.0168$ as displayed in Fig. 4 for

$$(7) \quad 11.11 C_A z^{0.5} P^{-1.5} = 0.0168 S_{B-C}^{1.08} \quad (n=39; r=0.98)$$

Solving equation (7) we obtain the paleo-productivity:

$$P^{1.5} = \frac{11.11 C_A z^{0.5} S_{B-C}^{-1.08}}{0.0168} = 660 C_A z^{0.5} S_{B-C}^{-1.08}$$

and

$$(8) \quad P = 72.6 C_A^{0.66} z^{0.32} S_{B-C}^{-0.71}$$

By definition, C_A can also be derived from the sediment properties, C , S_B , Φ and ρ :

$$(9) \quad C_A = C S_B \rho (1-\Phi) 10^{-1}$$

where $\rho (1-\Phi)$ is the dry bulk density.

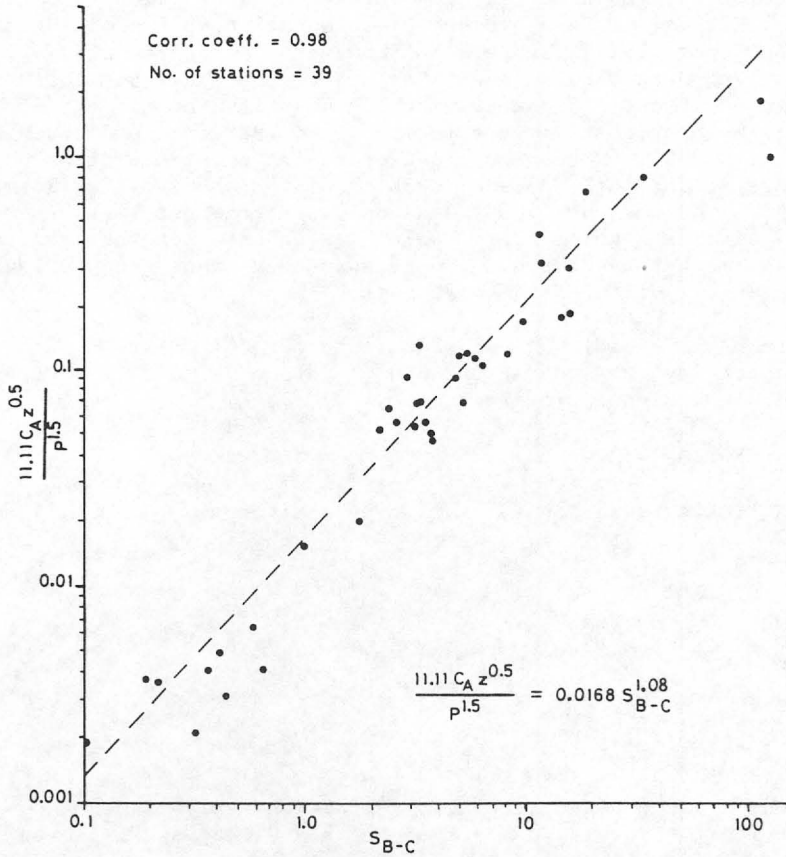


Figure 4. Presentation of the "Sealing Effect": Organic carbon accumulation rates (C_A) and water depths (z) normalized to primary production (P) as a function of the organic carbon free sedimentation rates (S_{B-C}).

Substituting equation (8) for the organic carbon accumulation rate (C_A) in equation (9) we obtain equation (10):

$$(10) \quad P = 15.9 C^{0.66} S_B^{0.66} (\rho(1-\Phi))^{0.66} S_{B-C}^{-0.71} z^{0.32}$$

In this equation, paleoproductivity (P) is measured in $\text{gcm}^{-2}\text{y}^{-1}$, organic carbon concentration (C) in weight percent, sedimentation rate (S_{B-C}) in $\text{cm } 1000\text{y}^{-1}$, water depth (z) in meters, density of sediment (ρ) in gcm^{-3} , and porosity of sediment (Φ) in percent water/100.

In order to test the validity of this equation, Fig. 5 compares measured primary productivity values (Table II) and modern paleoproductivity values as derived from surface sediment samples using equation (10). The values agree within a factor of 2 with a correlation coefficient of 0.80 ($n=39$).

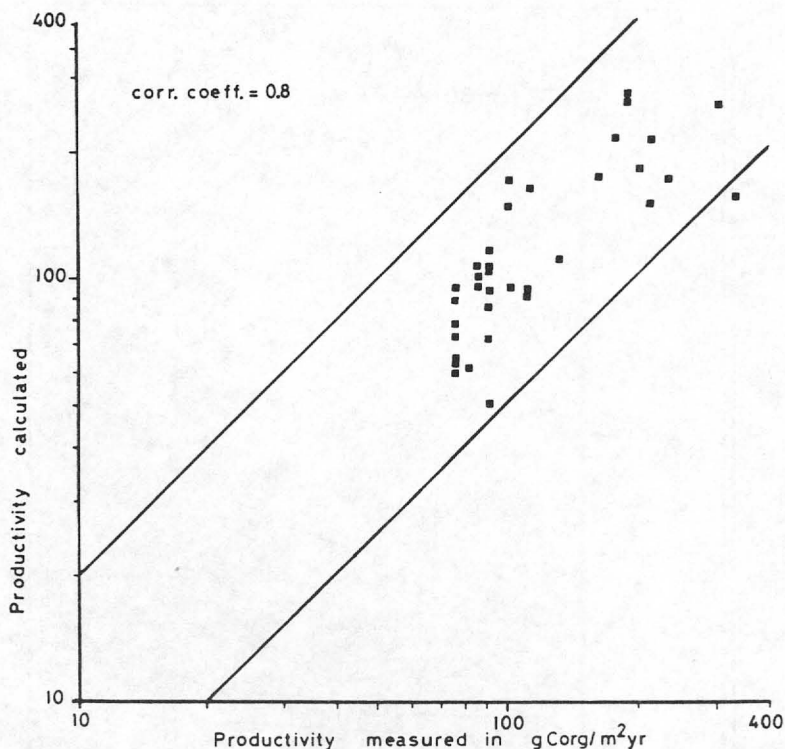


Figure 5. Measured values of surface primary productivity versus estimates calculated from equation (10) based on data in Table II. Most values agree within a factor of 2 or less, as shown by the bounding lines.

For estimating the Cretaceous ocean productivity, Stein (1986) recently used our approach (first presented at the 75th Annual Meeting of the Geologische Vereinigung; Sarnthein et al., 1985) and calculated P from equation (4) of Betzer et al. (1984), the "old" unscreened data set of Müller and Suess (1979) and lumped S_B and S_{B-C} . As a result, he arrived at equation (11), which is remarkably similar to equation (10).

$$(11) \quad P = 5.31 C^{0.71} S_B^{0.07} (\rho(1-\Phi))^{0.71} z^{0.45}$$

In addition to the variables contained in equation (10), a number of other factors may potentially control the preservation of carbon in the sediment. For example, Emerson (1985) presented a theoretical investigation of the roles of bottom water oxygen concentration, bioturbational mixing, and the carbon degradation rate (i.e., the susceptibility of carbon to degradation). Unfortunately, he did not describe the carbon preservation by means of carbon accumulation rates (C_A) but simply by organic carbon percentages (C). This variable does not compensate for manifold "dilution" effects by the non-carbon sediment supply and thus cannot be used as a measure of carbon flux, primary productivity

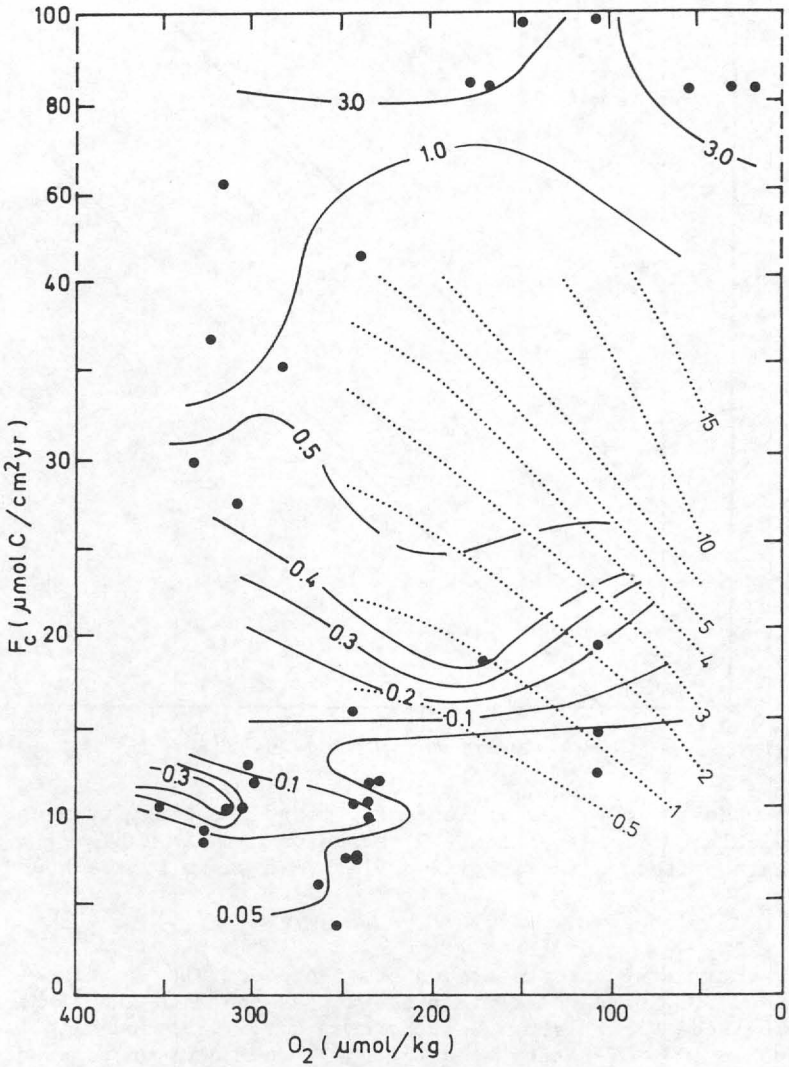


Figure 6. Lines of constant organic carbon accumulation rates as a function of particulate carbon flux C and bottom water oxygen concentrations (O_2). Dotted lines show (expected) content (%) of organic carbon calculated from the model of Emerson (1985).

ERRATUM

Estimated productivity values in Table II are based on equation (10) in the original form with powers to 4 decimal places.

$$\text{Prod} = 15.9342 * C^{0.6590} * S^{0.6590} * (p(1-\phi))^{0.6590} * S^{-0.7143} * Z^{0.3174}$$

B-C

Since acceptance of this paper, Equation (10) has been improved for a calculation of "New Productivity", by almost doubling the data set, and by subjecting the data to multiple regression analysis with total forcing (Sarnthein et al., Paleocceanography, in press).

rates or of carbon preservation (Müller and Suess, 1979). Hence we again tested the role of bottom-water oxygen concentration in the preservation of sedimentary organic carbon by illustrating the interdependence of C_A , F_C , and the bottom-water oxygen concentration (Fig. 6). The results are contrary to those predicted by Emerson (1985). C_A values equating to carbon preservation do not increase with decreasing O_2 concentration (dotted isolines in Fig. 6), because the oxidation of carbon continues as long as any free oxygen is available in bottom water. Only at O_2 concentrations below about 50-100 $\mu\text{mol/kg}$, accumulation rates of organic carbon tend to increase (Fig. 6, upper right corner).

In a similar manner, the relationship between organic carbon accumulation and bioturbation or the carbon degradation rate do not follow the trends suggested by Emerson (1985), if C_A values are employed instead of %C. The results are mostly contradictory, since they vary by a factor of up to 3 and 4 at a single site (Cochran, 1985), and accordingly, they are discarded.

Based on these findings, we decided to deduce our estimates of ocean paleoproductivity directly from equation (10). The regional applicability of this equation was tested by Tiedemann (1985, modified) who compared productivity data from surface sediments from a large range of different water depths and plankton hauls in the eastern equatorial Atlantic (Figs. 7a and b). The success of this test is largely the result of including the flux-water depth relationship into our paleoproductivity equation.

Finally, the productivity values calculated from equation (10) may be considerably biased because they are based on concentrations of sedimentary total organic carbon (%C), which lump together the proportions of organic matter that are derived from land and from marine plankton. Hydrogen index data from Rock-Eval pyrolysis indicate that terrigenous carbon may contribute as much as 60% of the carbon fraction in deep-sea sediments, especially offshore from river mouths and below dust trajectories (Tissot and Welte, 1984). However, routine quantification of the two different carbon sources is not yet possible by this method because it still contains too many caveats. Another approach to constrain the different sources of carbon is based on the very light $\delta^{13}\text{C}$ composition of land derived organic matter (-26‰) as compared to marine organic matter (-18 to -20‰) (Fontugne and Duplessy, 1978). Müller et al. (1983) calculated, as a worst-case estimate, a terrestrial contribution of 40% of the total sedimentary organic matter in modern sediments offshore from the exSpanish western Sahara. This value was considerably decreased during previous phases of enhanced marine plankton productivity, a variation which indicates a general, fairly constant background of dustborne carbon being overlain by a strongly fluctuating input of carbon from marine plankton. Because of a lack of pertinent data, unfortunately, we cannot distinguish between the different sources of carbon supply in this paper.

$\delta^{13}\text{C}$ Record of Benthic Foraminifera Tests

Zahn et al. (1986) demonstrated that the $\delta^{13}\text{C}$ data from different benthic foraminifera species carry different environmental signals as

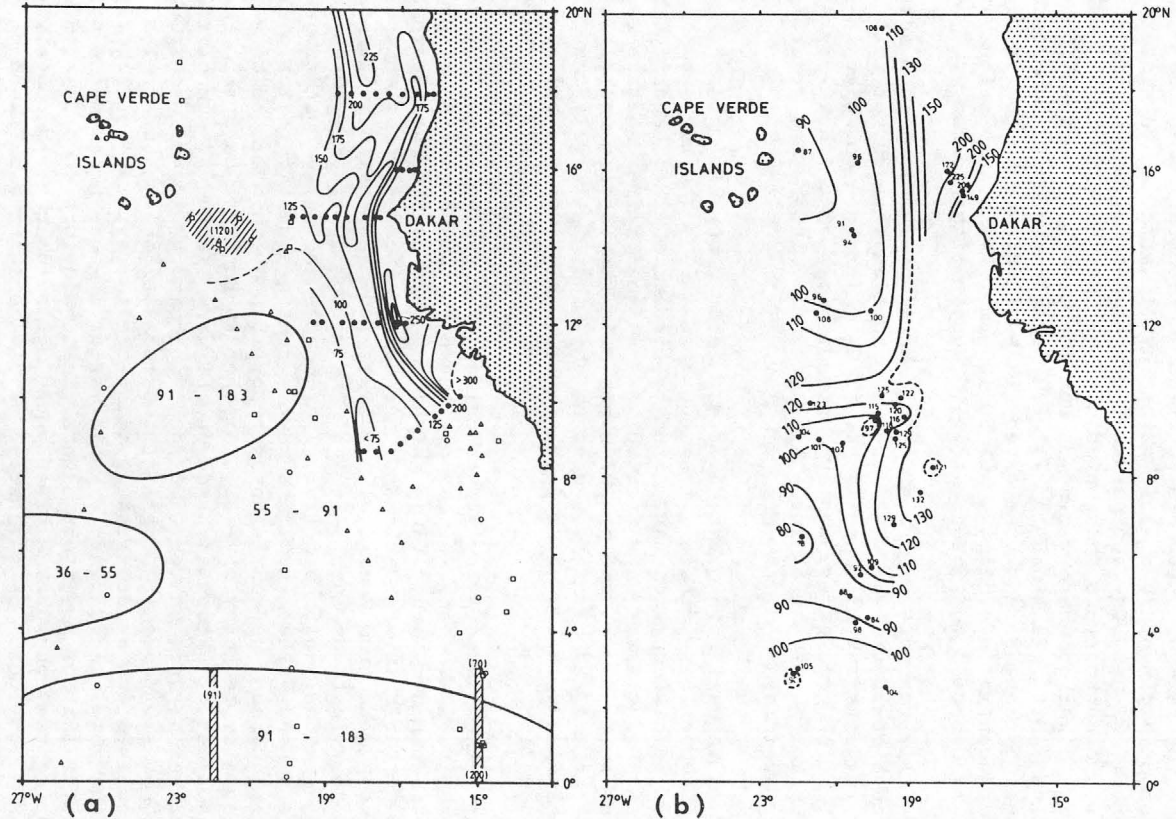


Figure 7. Regional distribution pattern of perennial surface primary productivity measured in the Equatorial East Atlantic (a) the pattern of estimates calculated from surface sediments by means of equation (10). (b) modified from Tiedemann, (1985).

the result of different foraminiferal microhabitats. On the one hand, the $\delta^{13}\text{C}$ record of the infaunal *Uvigerina peregrina/U. hollicki* group is strongly, although not linearly influenced by varying local accumulation rates of (isotopically light) carbon and thus, mainly by the local marine plankton production. On the other hand, the $\delta^{13}\text{C}$ values of the epifaunal species *C. wuellerstorfi* to a great extent reflect the large scale variations of total dissolved CO_2 in the ambient (regional) bottom water mass such as already postulated by Woodruff et al. (1980), Duplessy (1982), Duplessy et al. (1984) and Duplessy and Shackleton (1985).

Duplessy (op. cit.) mainly related such changes in dissolved CO_2 to fluctuating residence times of the deep water masses, but they can equally reflect fluctuations of ocean productivity (sensu P. Weyl in Broecker, 1982).

In this paper, we compare our paleoproductivity data with $\delta^{13}\text{C}$ curves from *C. wuellerstorfi*, which were measured at sediment cores from about 3000m water depth by Sarnthein et al. (1984) and Zahn et al. (1986). Based on the above reasoning, we regard these $\delta^{13}\text{C}$ curves as a bulk measure, a "memory" of the total CO_2 gradually accumulated from various high productivity cells in the ambient North Atlantic Deep Water (NADW) while it flows from its formation area in the North Atlantic to the south. Accordingly, we expect that an increase in surface ocean productivity (in addition to the effects of increasing NADW residence time) will result in overall reduced $\delta^{13}\text{C}$ values, and vice versa. Our $\delta^{13}\text{C}$ data were measured parallel with the $\delta^{18}\text{O}$ data.

Paleo-wind Strength

Trade winds are the main driving mechanism of low latitudinal oceanic upwelling. However, they control the plankton productivity and CO_2 transfer within upwelling regions only to a limited degree in a non-linear fashion (Codispoti, 1983). Other major factors are the original nutrient concentration of the upwelled source water and the perturbation of plankton blooms by excessive storminess, which may decrease the degree of carbon utilization.

Despite these complicating factors, it is tempting to evaluate paleo-wind speeds, because the relation between surface wind strength and (merely physical) coastal upwelling intensity is probably linear. This is suggested by the findings of Speth et al. (1978), who observed a linear connection between upwelling controlled zonal sea surface temperature (SST) anomalies and large-scale pressure gradients in the surface atmosphere off northwest Africa.

Paleo-wind speeds can be deduced from the grain-size distribution of aeolo-marine dust sediments based on a formula of Sarnthein et al. (1981). This calculation requires that both the thickness of the turbid atmospheric dust layer and the length of the dust trajectory from the shoreline to the sample location are known. However, the latter variable may be an indeterminant if the (trade) winds blow largely longshore such as offshore from northwest Africa. Here slight variations in wind direction and of sea level may result in large changes of the length of

the trajectory, a problem which can be only overcome by careful selection of the location of the sediment core.

RESULTS

Paleoproductivity Variations During the Last 140,000 Years

Fig. 8c presents two records of paleoproductivity change as calculated by equation (10) during the late Quaternary. The record of 'Meteor' core 12392 is derived from the outer influence range of an oceanic upwelling cell offshore from northwest Africa. This high-productivity region is one of the four major trade wind driven upwelling zones of the world ocean attached to an eastern (passive) continental margin (Fig. 3). The record of 'Meteor' core 13519 is obtained from the non-upwelling region of the Sierra Leone Rise, i.e. from an oceanic "desert" (Fig. 3).

In this "desert", the paleoproductivity only varied by 50 to 80% during the last 140,000 years, as compared to more than 300% in the vicinity of nearshore coastal upwelling. In both cores, low and approximately equal productivity levels of about $60-90 \text{ gC m}^{-2}\text{y}^{-1}$ generally occurred during interglacial stages, whereas high values are characteristic of glacial stages as depicted by the (benthos) $\delta^{18}\text{O}$ curve (Fig. 8d). High productivity also occurred in oxygen isotope stage 3, an intermediate state of climate which is poorly understood. In principle, these productivity variations were already recognized by Müller et al. (1983). Their data showed a clear signal of a 100,000 to 110,000 year productivity cycle, which can be traced as far back as approximately 500,000 years, and less distinctly, back to 750,000 years B.P. (Fig. 9).

Unlike the paleoproductivity curves, the $\delta^{13}\text{C}$ values of *C. wuellerstorfi* in core 13519 vary almost identically with those in core 12392 through time (Fig. 8a and b). In general, the two $\delta^{13}\text{C}$ curves correlate inversely with the strong fluctuations of paleoproductivity found in core 12392, but parallel those of core 13519 only to a limited extent. Likewise, the long-term 100,000 years productivity cycle of core 13519 can hardly be recognized on the $\delta^{13}\text{C}$ curve on Fig. 9.

Lowered $\delta^{13}\text{C}$ values of *C. wuellerstorfi* generally record a CO_2 enrichment in (here: North Atlantic) deep water (Duplessy, 1982). This enrichment may now be explained by a strongly increased flux of organic carbon from high productivity zones of coastal upwelling, as expected by our model. According to Duplessy (1982), an interglacial to glacial $\delta^{13}\text{C}$ decrease of about 0.8‰ (probably nearer 0.6 ‰) in the NADW should correspond to an additional 1150 GT (or 860 GT) of carbon stored away into the deep ocean (equal to about 150 years of the total new production; combined evidence of Koblentz-Mishke et al., 1970, and Platt and Harrison, 1985). Unfortunately, we cannot verify this number in terms of a paleoproductivity balance for the total north Atlantic or any other ocean, because these data are not yet available through last glacial and interglacial times. Nevertheless, the data obtained from core 12392 and other data sets from neighbouring cores along the east Atlantic continental margin (e.g., Müller et al., 1983, and other

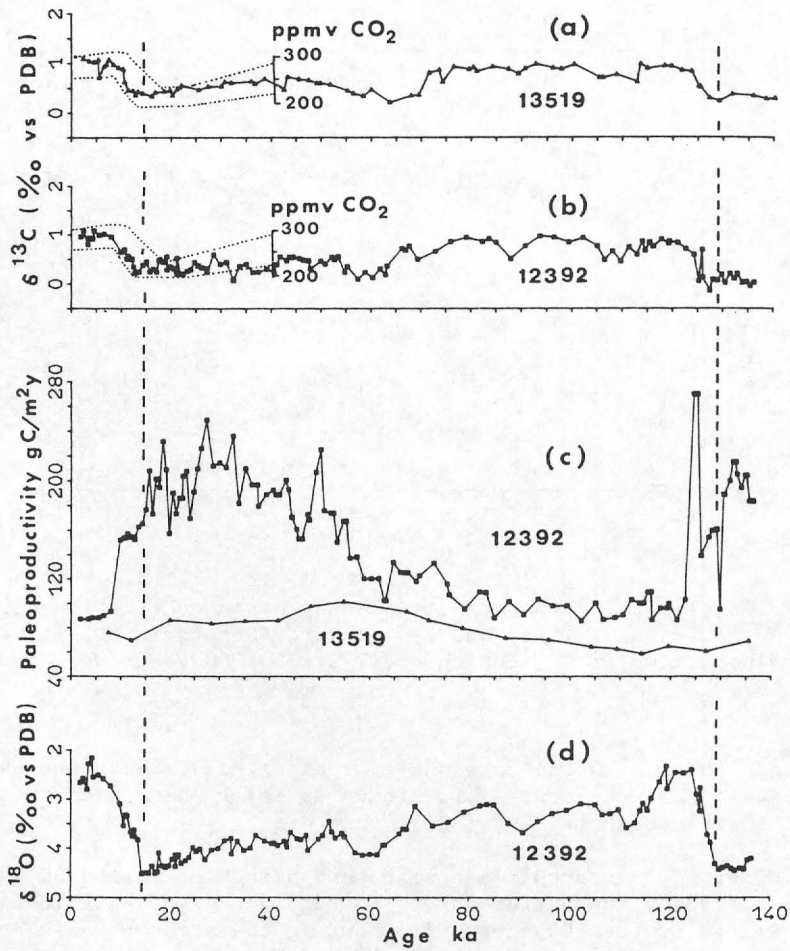


Figure 8. Late Quaternary changes in productivity during glacial and interglacial stages. The $\delta^{18}\text{O}$ curve of *Cibicidoides wuellerstorfi* in core 12392 largely reflects changes of global ice volume. The $\delta^{13}\text{C}$ curve measured from the same foraminifera specimens documents the total dissolved CO₂ content in ice cores (Neftel et al., 1982). Chronology of core 12392 after Thiede et al. (1982). Time scale of core 13519 after Herterich and Sarnthein (1984; modified).

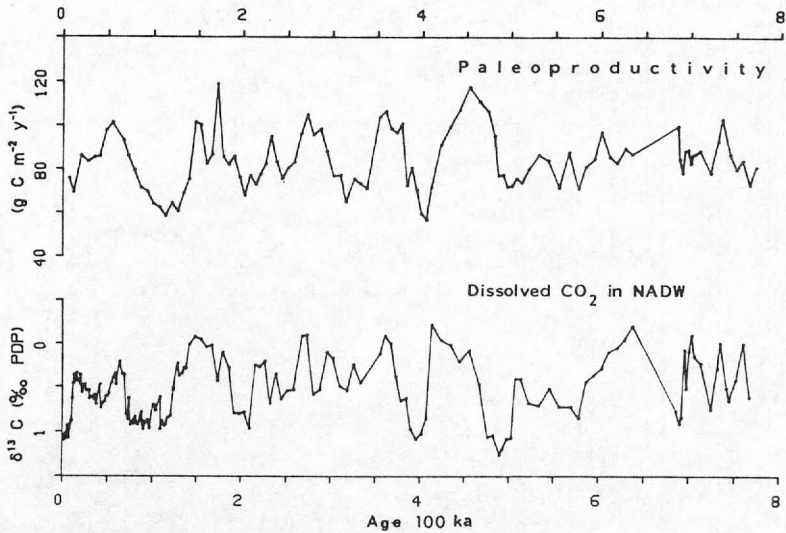


Figure 9. Cyclic paleoproductivity changes based on equation (10) and data of Müller et al. (1983) and $\delta^{13}\text{C}$ record (Sarnthein et al., 1984) of dissolved bottom water CO_2 during the last 750,000 years as recorded in core 13519.

unpublished data) make such a linkage highly likely, because coastal upwelling regions may be crucial for inducing major changes of the carbon transfer in the ocean (Flohn, 1983).

In order to test such a scenario, and using the method as Shackleton et al. (1983), the bottom water ^{13}C record of Fig. 8 is juxtaposed with the range of past CO_2 concentrations in the atmosphere as estimated by Neftel et al. (1982) from ice core data (Fig. 1). The scales of atmospheric CO_2 and $\delta^{13}\text{C}$ are positioned on the assumption that the ^{13}C difference observed at the top of the core reflects a pre-anthropogenic atmospheric CO_2 level of about 280 ppmv. The scales are adjusted using Broecker's (1982) model to scale the isotopic range for an implied record of surface-water (!) CO_2 content. In Fig. 8, the range of atmospheric CO_2 variations indeed appears entirely consistent with the ^{13}C record of bottom water CO_2 . The last glacial to interglacial increase of atmospheric CO_2 by about 50% (100 ppmv, equal to 230 GT carbon) parallels the outlined (almost four fold) 860 GT decrease of carbon in the NADW (Duplessy, 1982, modified) and perfectly matches the abrupt reversal of productivity in the coastal upwelling zone. Three quarters of the carbon lost by the deep water were probably added to the concentration in the (1000m thick) ocean surface water, and 1/4 to the atmosphere.

Flohn (1986) estimated a similar order of magnitude for the CO_2 exchange as controlled by oceanic productivity in upwelling regions during modern interannual variations of atmospheric pCO_2 .

PHASE RELATIONSHIPS DURING GLACIAL TERMINATIONS I AND II

Temporal leads and lags across climatic reversals provide an important tool for identifying the cause-effect relationships and the external forcing mechanisms controlling (abrupt?) climatic change. Based on its high sedimentation rates (7-10 cm/1000y) and the large number of climatic proxy data already determined, core 12392 gives an excellent opportunity to test, in detail, the phase relationships between changes of paleoproductivity, bottom water and atmospheric pCO_2 , and global deglaciation during the last two Terminations.

The onset of Glacial Terminations is defined by a sudden and long term turn in the (benthos) oxygen isotope curve towards lighter values indicative of large-scale glacial melting and global sea level rise (Fig. 8) (Broecker and van Donk, 1970; Ruddiman and McIntyre, 1976). To facilitate discussion, the onset ages of the various steps of Terminations I and II in core 12392 are summarized in Table I and compared with the age of turning points (also stepwise) in the history of productivity and bottom water CO_2 during this time.

Broecker (1982) related the general decrease of ocean paleoproductivity during deglaciation time to limited phosphate and nitrate reservoirs and ultimately to the sea level rise and a flooding of the shelf. However, it is clear from Fig. 8 and Table I that the onset of the massive decrease was either synchronous with the start of both Terminations I and II or occurred slightly earlier. Hence, the decrease in paleoproductivity cannot be the result of glacial melt and sea-level rise. However, the apparent 1500-year lead of the productivity decrease over glacial melting, as suggested at Terminations IA and IIA, may also be incorrect. The deep (early) position of the turning point in paleoproductivity may be caused by post-depositional processes. Possibly, bioturbation lowered the carbon concentration to sediment depths below the actual reversal by the consumption of "fossil" carbon as soon as the contemporaneous flux of carbon to the sea floor was reduced. The 1,500 years lead under discussion (Table III) corresponds to about 15cm sediment thickness, which perhaps would still be accessible to consumption by bioturbational mixing (Rowe, 1985).

Of course, it is legitimate to question the extent to which phase relationships observed in a single core (although obtained from a key location) have general implications, at least for one major upwelling region. For example, the turning point of the paleoproductivity curve at 18,200 y B.P., which is problematic in core 12392, forms the only dominant event in the paleoproductivity record of core 16415 near the southern margin of the same east Atlantic coastal upwelling region, at about $10^\circ N$ (Fig. 10) and also in core 13519 (Fig. 8). Thus, only a future regional integration of different records will provide a final answer to the exact timing of the paleoproductivity event. For example, Legeckis (1986) depicts contrasting occurrences of El Niño situations in the equatorial Atlantic and the eastern Pacific. However, its full synchronicity or even its lead to global ice melt can already be obtained from the present data.

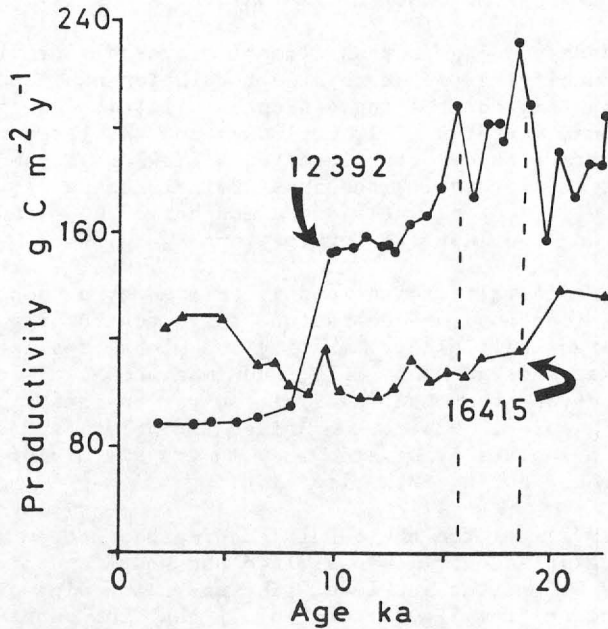


Figure 10. Paleoproductivity record of core 16415. Estimates calculated from equation (10) based on data and stratigraphy of Vogelsang (1985).

During Terminations I and II, the respective reversals in the $\delta^{13}\text{C}$ record began (in both cores!) markedly later than those of oxygen isotopes and of paleoproductivity, with a time lag of 2,000 to 4,500 years (Fig. 8; Table I). This result also may strongly affect existing models. Broecker et al. (1985) and Boyle and Keigwin (1985) expected that primarily, an increased formation of NADW gave rise to the large emission of CO_2 from the deep ocean to the atmosphere during deglaciation phases and thereby possibly enhanced the "abrupt" climatic change.

The phase relationships depicted in Fig. 8 however suggest that the CO_2 emission was probably the result of several thousand years of reduced upwelling productivity in low latitudes and diminished CO_2 extraction from the atmosphere. Such a mechanism is in harmony with the ice core record of past atmospheric CO_2 concentrations (Fig. 8). These concentrations had already increased after 16,500 y B.P., which was several thousand years prior to the increase of benthos $\delta^{13}\text{C}$, but about synchronous with the reduction of upwelling productivity. Unlike the atmospheric CO_2 reservoir, that of the deep ocean just emerges as a slow system with a delayed response to a quickly changing forcing by ocean productivity at the sea surface.

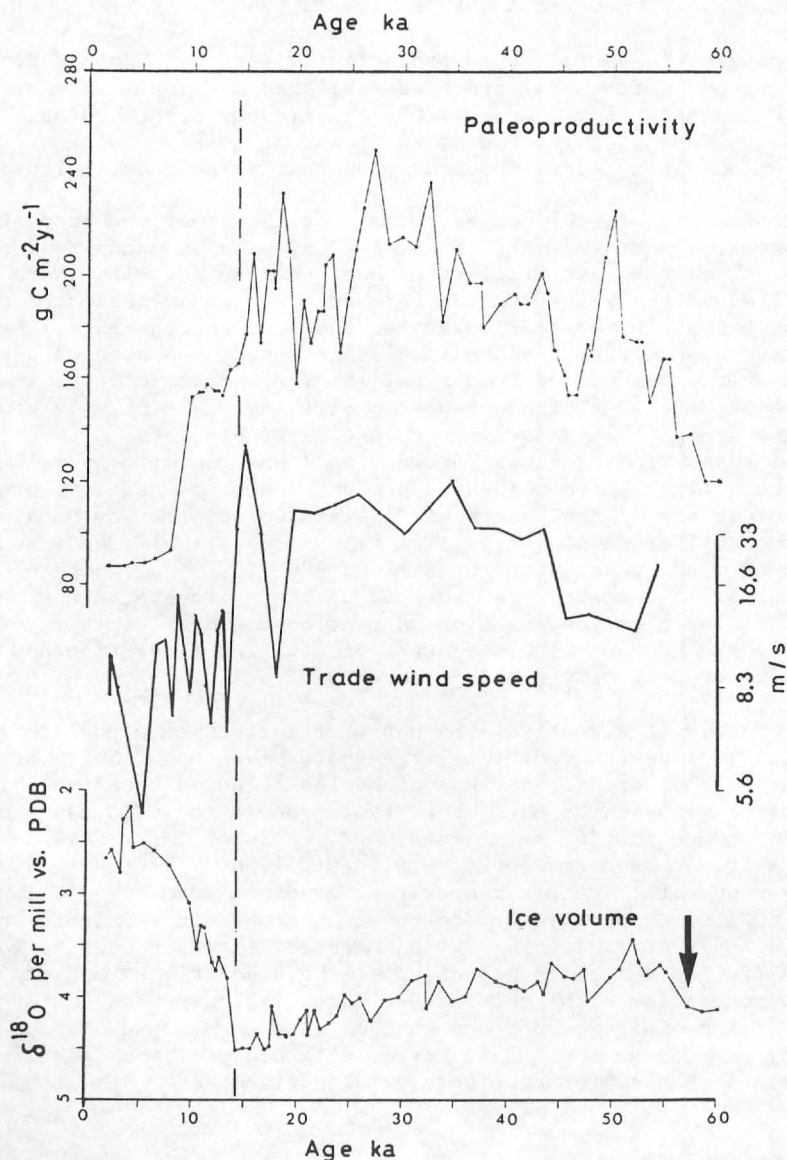


Figure 11. Paleoproductivity and $\delta^{18}\text{O}$ record of global ice volume measured in core 12392 versus the history of average trade wind speeds (u). Approximative dust storm wind speeds were calculated from an equation of Sarnthein et al. (1981) and based on grain size data from aeolo-marine dust deposits in core 13289 (Koopmann, 1981) and on the assumption of an almost constant thickness of the turbid atmospheric dust layer (1.2km) and a constant length of dust transport from the shoreline (about 200km).

POSSIBLE ORIGIN OF UPWELLING PRODUCTIVITY CHANGES

Changes of coastal ocean productivity (and the "Rain Ratio Model" of Berger and Keir, 1984) appear established as a prime factor for the massive increase of atmospheric CO₂ synchronous or preceding the global ice melt. Consequently, the focus of our discussion must shift to the question of which factor induced the abrupt paleoproductivity changes.

Labracherie (1980) demonstrated that the upwelling productivity offshore from northwest Africa was increased by an unknown order of magnitude during the last glaciation, because nutrient-rich South Atlantic Central Water (SACW) penetrated farther north as suggested by the frequency of certain radiolarian tracer species. Furthermore, the intensity of the upwelling process itself increased by about 50% during glacial times as deduced from zonal sea surface temperature anomalies (Sarnthein, 1982). This enhanced upwelling appears clearly coupled with enhanced synglacial trade wind speeds (Sarnthein et al., 1982). A continuous speed record across Termination I was tentatively calculated from the well dated core 13289. Its dust deposits are little affected by fluctuations of the length of dust trajectory (rather by a mixture of dust from different sources) (Fig. 11) and reveal a marked, sudden decrease of wind speeds starting near 14,900 y B.P., although one cannot take literally the absolute range of 35-5 m/s because of the many possible pitfalls in the calculation as mentioned above. This event is remarkably synchronous with the onset of global deglaciation and the decrease of productivity found in core 12392.

Possibly, the sensitive response of meridional wind strength to deglaciation was induced by a large-scale break-up of North Atlantic sea ice during the very first phase of deglaciation, a break-up which in turn may have been the most sensitive response to an increase of the insolation budget during this time (Ruddiman and McIntyre, 1981). At least seasonal open-sea conditions in middle high latitudes will effectively reduce the oceanic temperature gradient from high to low latitudes and thus, quickly lead to decreasing meridional winds, which compensate for this gradient. By this mode of interaction, the synchronous change (in geological terms) of upwelling productivity and atmospheric CO₂ concentration with the onset of deglaciation can be easily explained as joint immediate response to changes in the solar insolation regime and may provide an important, highly flexible positive (non-linear) feedback mechanism for accelerating climatic change.

ACKNOWLEDGEMENTS

The authors greatly appreciate the many helpful and stimulating discussions with Erwin Suess, Peter Müller, Wolfgang Berger, Wallace S. Broecker, and Helmut Erlenkeuser and the careful review of this paper by W.H. Berger, H. Flohn, and L. Mayer. This work was supported by the National Program of Climate Research of the Federal Republic of Germany (Grant No. 5138391-KF20041 of the Ministry of Research and Technology)

REFERENCES

- Arrhenius, S., 1896. On the influence of carbonic acid in the air upon the temperature of the ground, *Phil. Mag.*, 41: 437.
- Berger, W.H. and Johnson, R.F., 1978. On the thickness and the ^{14}C age of the mixed layer in deep-sea carbonates, *Earth Planet. Sci. Lett.*, 41: 223-227.
- Berger, W.H. and Keir, R.S., 1984. Glacial-Holocene changes in atmospheric CO_2 and the deep-sea record. In: *Climate Processes and Climate Sensitivity*, edited by J.E. Hansen and T. Takahashi, *Geophys. Monogr.*, 29 (AGU, Washington D.C.), 337-351a.
- Betzler, R.R., Showers, W.J., Laws, E.A., Winn, C.D., DiTullio, G.R. and Kroopnick, P.M., 1984. Primary productivity and particle fluxes on a transect of the equator at 153°W in the Pacific Ocean, *Deep-Sea Res.*, 31 (1): 1-11.
- Boyle, E.A., 1986. Paired cadmium and carbon isotope data in benthic foraminifera: Implications for changes in oceanic phosphorus, oceanic circulation, and atmospheric carbon dioxide, *Geochim. Cosmochim. Acta*, 50: 265-276.
- Boyle, E.A. and Keigwin, L.D., 1985. Comparison of Atlantic and Pacific paleo-chemical records for the last 215,000 years: Changes in deep ocean circulation and chemical inventories, *Earth Planet. Sci. Lett.*, 76 (1/2): 135-150.
- Broecker, W.S., 1982. Glacial to interglacial changes in ocean chemistry. In: *Climatic variability in the oceans*, edited by E.B. Kraus and H.P. Hansen, *Prog. Oceanogr.*, 11: 151-197.
- Broecker, W.S. and van Donk, J., 1970. Insolation changes, ice volumes and the ^{18}O record in deep-sea sediments, *Rev. Geophys. Space Phys.*, 8: 169-198.
- Broecker, W.S., 1984. Carbon cycle: Carbon dioxide circulation through ocean and atmosphere, *Nature*, 308: 602.
- Broecker, W.S. and Peng, T.-H., 1986. Carbon Cycle: 1985, Glacial to interglacial changes in the operation of the global carbon cycle, *Radiocarbon*, 28 (2A): 309-327.
- Broecker, W.S., Peteet, D.M. and Rind, D., 1985. Does the ocean-atmosphere system have more than one stable mode of operation?, *Nature*, 315: 21-26.
- Codispoti, L.A., 1983. On nutrient variability and sediments in upwelling regions. In: *Coastal Upwelling. Its Sediment Record*, A, edited by E. Suess and J. Thiede (Plenum Press, New York), 125-146.
- Cochran, J.K., 1985. Particle mixing rates in sediments of the eastern equatorial Pacific: Evidence from ^{210}Pb , 239 , ^{240}Pu and ^{137}Cs distributions at MANOP sites, *Geochim. Cosmochim. Acta*, 49: 1195-1210.
- Delmas, R.J., Ascensio, J.-M. and Legrand, M., 1980. Polar ice evidence that atmospheric CO_2 20,000 yr BP was 50% of present, *Nature*, 284: 155-157.
- Duplessy, J.-C., 1982. North Atlantic Deep Water circulation during the last-climatic cycle, *Bull. Inst. Geol. Bassin d'Aquitaine, Bordeaux*, 31: 379-391.
- Duplessy, J.C., Shackleton, N.J., Matthews, R.K., Prell, W., Ruddimann, W.F., Caralp, M. and Hendy, C.H., 1984. ^{13}C record of benthic foraminifera in the last Interglacial ocean: Implications for the

- carbon cycle and the global deep water circulation, *Quat. Res.*, 21 (2): 244-263.
- Duplessy, J.C., Labeyrie, L.L. and Shackleton, N.J., 1985. The oxygen isotope record of benthic foraminifera: Effect of deep water temperature and ice volume changes, *EOS*, 66 (18).
- Duplessy, J.-C. and Shackleton, N.J., 1985. Response of global deep-water-circulation to Earth's climatic change 135,000-107,000 years ago, *Nature*, 316: 500-507.
- Emerson, S., 1985. Organic carbon preservation in marine sediments. In: *The carbon cycle and atmospheric CO₂: Natural variations Archean to Present*, edited by E.T. Sundquist and W.S. Broecker, *Geophys. Monogr.*, 32 (AGU Washington D.C.), 78-87.
- Erlenkeuser, H., 1980. ¹⁴C age and vertical mixing of deep-sea sediments. A comment on a paper of Berger and Johnson (1978), *Earth Planet. Sci. Lett.*, 47: 319-126.
- Flohn, H., 1983. A climate feedback mechanism involving oceanic upwelling, atmospheric CO₂ and water vapour. In: *Variations in the Global Water Budget*, edited by Street-Perrot et al. (D. Reidel Publ. Co., Dordrecht, Holland), 403-418.
- Flohn, H., 1986. Singular events and catastrophes now and in climatic history, *Naturwissenschaften* 73: 136-149.
- Fontugne, M. and Duplessy, J.C., 1978. Carbon isotope ratio of marine plankton related to surface water masses, *Earth Planet. Sci. Lett.*, 41 (3): 365-371.
- Grassl, H., Maier-Reimer, E., Degens, E.T., Kempe, S. and Spitzky, A., 1984. CO₂, Kohlenstoff-Kreislauf und Klima, I. Globale Kohlenstoffbilanz, *Naturwissenschaften*, 71: 129-136.
- Hasselmann, K., 1976. Stochastic climate models, I, *Tellus*, 28: 473.
- Herterich, K. and Sarnthein, M., 1984. Brunhes time scale: Tuning by rates of calcium-carbonate dissolution and cross spectral analyses with solar insolation. In: *Milankovitch and Climate*, I, edited by A. Berger et al. (D. Reidel Publ. Co., Dordrecht, Holland), 447-466.
- Imbrie, J., Hays, J.D., Martinson, D.G., McIntyre, A., Mix, A.C., Morley, J.J., Pisias, N.G., Prell, W.L. and Shackleton, N.J., 1984. The orbital theory of Pleistocene climate: Support from a revised chronology of the marine $\delta^{18}\text{O}$ record. In: *Milankovitch and Climate* (D. Reidel Publ. Co., Dordrecht, Holland), 269-305.
- Koblentz-Mishke, O.J., Volkovinsky, V.V. and Kabanova, J.G., 1970. Plankton primary production of the World Ocean. In: *Scientific Exploration of the South Pacific*, edited by W.S. Wooster, 183-193.
- Koopmann, B., 1981. Sedimentation von Saharastaub im subtropischen Atlantik während der letzten 25,000 Jahre, *'Meteor' Forsch. Ergeb. C* 35: 23-59.
- Labracherie, M., 1980. Les Radiolaires temoins de l'évolution hydrologique depuis le dernier maximum glaciaire au large du Cap Blanc (Afrique du Nord-Ouest), *Palaeogeogr. Palaeoclimatol. Palaeoecol.*, 32 (1/2): 163-184.
- Legeckis, R., 1986. Tropical changes at the sea surface, *Nature*, 322: 15.
- Müller, P.J., Erlenkeuser, H. and von Grafenstein, R., 1983. Glacial-Interglacial cycles in oceanic productivity inferred from organic carbon contents in eastern North Atlantic sediment cores. In:

- Coastal Upwelling: Its Sediment Record, B.* edited by J. Thiede and E. Suess (Plenum Press, New York), 365-398.
- Müller, P.J. and Suess, E., 1979. Productivity, sedimentation rate and sedimentary organic matter in the oceans - I Organic carbon preservation, *Deep-Sea Res.*, 26: 1347-1362.
- Neftel, A., Oeschger, H., Schwander, J., Stauffer B. and Zumbunn, R., 1982. Ice core sample measurements give atmospheric CO₂ content during the past 40,000 years, *Nature*, 295: 220-223.
- Oudot, C. and Andrie, C., 1986. Pressions partielles de CO₂ dans l'Atlantique tropicale: variabilité dans les eaux de surface et dans l'atmosphère en janvier et juillet 1983, *Oceano. Acta*, 9 (2), in press.
- Pedersen, T.F., 1983. Increased productivity in the eastern equatorial Pacific during the last glacial maximum (19,000 to 14,000 yr B.P.), *Geol.*, 11: 16-19.
- Peltier, W.R. and Hyde, W., 1984. A model of the ice age cycle. In: *Milankovitch and Climate*, edited by A. Berger et al. (D. Reidel Publ. Co., Dordrecht, Holland), 565-580.
- Platt, T. and Harrison, W.G., 1985. Biogenic fluxes of carbon and oxygen in the ocean, *Nature*, 318: 55-58.
- Reimers, C.E. and Suess, E., 1983a. Late Quaternary fluctuations in the cycling of organic matter off central Peru: A proto-kerogen record. In: *Coastal Upwelling. Its Sediment Record. A*, edited by E. Suess and J. Thiede (Plenum Press, New York), 497-526.
- Reimers, C.E. and Suess, E., 1983b. Spatial and temporal patterns of organic matter accumulation on the Peru continental margin. In: *Coastal Upwelling Record, B*, edited by E. Suess and J. Thiede (Plenum Press, New York), 311-346.
- Rowe, G.T., 1985. The biological fate of organic matter on the NE US continental margin - SEEP Area, 1983/84, *EOS*, 66 (18), 283.
- Ruddiman, W.F. and McIntyre, A., 1976. Northeast Atlantic paleoclimatic changes over the past 600,000 years, *Geol. Soc. Am. Mem.*, 145: 11-146.
- Ruddiman, W.F. and McIntyre, A., 1981. The North Atlantic Ocean during the last deglaciation, *Palaeogeogr. Palaeoclimatol. Palaeoecol.*, 35: 145-214.
- Sarnthein, M., 1982. Zur Fluktuation der subtropischen Wüstengürtel seit dem letzten Hochglazial vor 18,000 Jahren: Klimahinweise und -modelle aus Tiefseesedimenten, *Geomethodica*, 7: 125-161.
- Sarnthein, M., Erlenkeuser, H., von Grafenstein, R. and Schröder, C., 1984. Stable isotope stratigraphy for the last 750,000 years; 'Meteor' core 13519 from the eastern equatorial Atlantic', *'Meteor' Forsch. Ergeb. C* 38: 9-24.
- Sarnthein, M., Erlenkeuser, H. and Zahn, R., 1982. Termination I: The response of continental climate in the subtropics as recorded in deep-sea sediments, *Bull. Inst. Geol. Bassin d'Aquitaine*, 31: 393-407.
- Sarnthein, M., Tetzlaff, G., Koopmann, B., Wolter, K. and Pflaumann, U., 1981. Glacial and interglacial wind regimes over the eastern subtropical Atlantic and NW Africa, *Nature*, 293: 193-196.
- Sarnthein, M., Winn, K. and Zahn, R., 1985. Paleoproductivity and the effect of oceanic upwelling on atmospheric CO₂ during Glacial and Interglacial times, *Terra Cognita*, 5 (1): 82.

- Shackleton, N.J., 1977. The oxygen isotope stratigraphic record of the Late Pleistocene, *Phil. Trans. Roy. Soc. Lond.*, B 280: 169-182.
- Shackleton, N.J., Hall, M.A., Line, J. and Shuxi, C., 1983. Carbon isotope data in core V 19-30 confirm reduced carbon dioxide concentration in the ice age atmosphere, *Nature*, 306: 319-322.
- Shackleton, N.J. and Opdyke, N.D., 1973. Oxygen isotope and paleomagnetic stratigraphy of equatorial Pacific core V 28-238: Oxygen isotope temperatures and ice volumes on a 10^5 year scale, *Quat. Res.*, 3: 39-55.
- Siegenthaler U. and Wenk, Th., 1984. Rapid atmospheric CO₂ variations and ocean circulation, *Nature*, 308: 624-625.
- Speth, P., Detlefsen, H. and Sierts, H.-W., 1978. Meteorological influence on upwelling off northwest Africa, *Dt. hydrogr. Zt.*, 31 (3): 95-104.
- Stein, R., 1986. Surface-water productivity as inferred from sediments deposited in oxic and anoxic deep-water environments of the Mesozoic Atlantic. In: *Proc. of Blackshale Conference*, Hamburg, 1985, edited by E. Degens, 20 ms-p, in press.
- Suess, E., 1980. Particulate organic carbon flux in the oceans - Surface productivity and oxygen utilization, *Nature*, 288: 260-263.
- Thiede, J., Suess, E. and Müller, P.J., 1982. Late Quaternary fluxes of major sediment components to the sea floor at the northwest African continental slope. In: *Geology of the northwest African continental margin*, edited by U. v. Rad et al. (Springer, Heidelberg), 605-631.
- Tiedemann, R., 1985. Verteilung von organischem Kohlenstoff in Oberflächen-sedimenten und die örtliche Primärproduktion im äquatorialen Ostatlantik, 0-20°N, 15-25°W, *Unpubl. M.Sc. Thesis*, Kiel Univ., 74 pp.
- Tissot, B.P. and Welte, D.H., 1984. *Petroleum Formation and Occurrence*, Springer, Berlin, 2nd edition.
- Vogelsang, E., 1985. Hochauflösende Zeitreihen der Termination I aus Sedimenten des äquatorialen Ostatlantiks, *Unpubl. M.Sc. Thesis*, Kiel Univ., 85 pp.
- Woodruff, F., Savin, S.M. and Douglas, R.G., 1980. Biological fractionation of oxygen and carbon isotopes by recent benthic foraminifera, *Mar. Micropaleont.*, 5: 3-11.
- Zahn, R., Winn, K. and Sarnthein, M., 1986. Benthic foraminiferal $\delta^{13}\text{C}$ and accumulation rates of organic carbon: *Uvigerina peregrina* group and *Cibicidoides wuellerstorfi*, *Paleoceanogr.*, 1 (1): 27-42.

TABLE I

Organic carbon flux rates in the water column and mean "surface" primary production rates compiled from data sets of Suess (1980), Smith and Hinga (1983) and Emerson (1985).

Latitude (°)	Longitude (°)	Water Depth (m)	Carbon flux ($\text{gm}^{-2} \text{yr}^{-1}$)	Primary production ($\text{gm}^{-2} \text{yr}^{-1}$)
31.5 N	55.9 W	976	0.89	40
31.5 N	55.9 W	3694	0.32	40
31.5 N	55.0 W	5367	0.45	45
13.5 N	54.0 W	389	2.46	50
13.5 N	54.0 W	988	1.44	50
13.5 N	54.0 W	3755	0.63	50
13.5 N	54.0 W	5068	0.62	50
15.3 N	151.5 W	378	1.30	40
15.3 N	151.5 W	2778	0.40	40
15.3 N	151.5 W	4280	0.32	40
15.3 N	151.5 W	5582	0.24	40
32 nm SE	Bermuda	3200	0.77	40
0.6 N	86.1 W	2650	2.28	100
27.7 N	78.9 W	675	2.60	72
33.5 N	76.2 W	1345	5.40	85
38.3 N	69.6 W	3650	4.20	160
24.9 N	77.7 W	2000	2.10	72
36.7 N	122.2 W	50	158.00	500
36.7 N	122.2 W	250	92.00	500
36.7 N	122.2 W	700	42.00	500
36.7 N	122.2 W	50	33.00	150
36.7 N	122.2 W	250	19.00	150
36.7 N	122.2 W	700	17.00	150
32.8 N	144.4 W	75	25.00	100
32.8 N	144.4 W	575	5.30	100
32.8 N	144.4 W	1050	4.40	100
38.8 N	72.5 W	2200	6.30	100
38.5 N	72.0 W	2750	2.30	160
55.6 N	15.4 E	55	65.00	305
15.1 S	75.4 W	50	240.00	1200
15.1 S	75.5 W	70	130.00	600
15.1 S	75.5 W	100	110.00	600
6.6 N	92.8 W	3500	1.44	91
8.8 N	104.0 W	3100	1.68	108
34.0 N	65.8 W	5140	0.72	72
32.5 N	117.8 W	1193	9.80	273
32.3 N	117.5 W	1230	9.80	273
32.5 N	120.6 W	3815	9.80	307

TABLE II

Core data used in the derivation of the productivity formula

Core No./ Station	Water depth (m)	C %	ρ (1- Φ) g/cm ³	S _B cm/ka	S _{B-C} cm/ka	C _A g/m ² yr	Productivity	
							measured g/m ² yr	estimated g/m ² yr
12392-1	2575	0.35	0.9780	5.05	5.02	0.17286	75	87
12310-3	3076	0.34	0.6504	3.80	3.78	0.08403	90	70
12327-4	2037	1.34	0.4065	8.33	8.14	0.45374	130	108
12328-4	2798	1.66	0.5691	15.08	14.65	1.42462	230	167
12329-4	3315	0.61	0.6233	2.56	2.54	0.09733	90	105
12336-1	3645	0.44	0.6775	2.20	2.18	0.06558	75	93
12337-4	3085	1.46	0.5691	4.90	4.78	0.40713	160	168
12344-3	711	2.59	0.5691	16.45	15.73	2.42468	210	146
12345-4	966	3.67	0.5691	16.45	15.43	3.43574	210	206
12347-1	2710	2.34	0.5691	12.48	11.98	1.66195	175	212
13209-2	4713	0.51	0.5691	3.20	3.17	0.09288	85	98
13521-1	4504	0.37	0.6450	3.50	3.48	0.08353	90	84
16017-2	812	1.81	0.9879	6.80	6.68	1.21591	200	179
16402-1	4203	0.46	0.6037	5.24	5.20	0.14552	110	89
16403-2	4234	0.45	0.6310	3.66	3.63	0.10393	110	92
16404-1	4787	0.42	0.6460	3.17	3.15	0.08601	95	94
16405-1	4870	0.43	0.7501	3.40	3.37	0.10966	95	105
16415-1	3841	0.61	0.6500	2.70	2.67	0.10705	90	114
16432-2	4515	0.52	0.6447	5.40	5.35	0.18103	90	103
V15-141	5934	0.72	0.6500	2.90	2.86	0.13572	100	145
V15-142	5885	0.92	0.6500	3.30	3.25	0.19734	100	169
10127-2	5686	0.28	0.3710	0.19	0.19	0.00197	50	61
10132-1	5004	0.22	0.5300	0.58	0.58	0.00676	75	60
10140-1	5144	0.33	0.3735	0.41	0.41	0.00505	75	64
10141-1	5189	0.31	0.3735	0.36	0.36	0.00417	75	62
10145-1	4599	0.21	0.5300	0.32	0.32	0.00356	100	58
10147-1	4619	0.23	0.5300	0.43	0.43	0.00524	100	61
10175-1	5164	0.40	0.3968	0.23	0.23	0.00365	75	78
7706-37	370	13.20	0.2702	50.00	34.10	17.83320	185	255
7706-39	186	13.20	0.2268	160.00	126.62	47.90016	330	154
7706-41	411	19.60	0.1910	160.00	112.47	59.89760	330	250
7706-44	580	7.83	0.4880	13.00	11.33	4.96735	185	278
7706-49	3970	3.23	0.2300	20.00	18.91	1.48580	110	160
7706-50	4902	0.78	0.3500	6.00	5.92	0.16380	90	92
7610-08	2060	1.50	0.2904	10.00	9.74	0.43560	100	93
MANOP H	3500	0.90	0.1130	0.66	0.65	0.00671	90	49
MANOP M	3100	1.20	0.1700	1.00	0.98	0.02040	75	73
MANOP C	4450	0.36	0.3820	1.80	1.79	0.02475	80	60
MANOP S	4915	0.90	0.2240	0.10	0.10	0.00202	75	94

TABLE III

Interpolated ages (y B.P.) of major turning points in the $\delta^{18}\text{O}$ deglaciation record, the productivity history of coastal upwelling, and in the $\delta^{13}\text{C}$ record of deep-water CO_2 concentration as measured in Meteor core 12392. Age estimates of the last 30,000 years are largely based on radiocarbon ages of planktonic foraminifera larger than 125m.

$\delta^{18}\text{O}$ (<i>C.wuellerstorfi</i>)	Onset of Paleoproductivity decrease	Onset of $\delta^{13}\text{C}$ increase (<i>C.wuellerstorfi</i>)
Onset Termination I		
Step B: 10,500	9,800	
Step A: 14,250 ¹	15,700	12,700 ⁵
	?18,400 ³	
Onset Termination II		
Step B: 125,000 ²	124,500 ⁴	
Step A: 130,000 ²	131,700	127,400 ⁵

1) This turning point is about 1,500 years younger than that found in a well dated, high-resolution sediment core 700km further further south (Sarnthein et al., 1982), but similar to that of core 13519.

2) By analogy with Ruddiman & McIntyre (1976) and Imbrie et al. (1984).

3) Identification ambiguous, because it is based only on a single measurement.

4) A preceding intra-Termination productivity culmination near 125,000 y B.P. is regarded as real because it is supported by independent tantamount evidence from a synchronous, extreme $\delta^{13}\text{C}$ minimum of *Uvigerina peregrina* (Zahn et al., 1986).

5) Only a single turning point occurs in each Termination.